

Power Control in PV Systems for EV Charge Optimization

Md Shahnawaz Khan ^{#1}, Chirag Gupta ^{*2}, Abhimanyu Kumar ^{#3}

[#]M.Tech Scholar & Electrical Department & RKDF University
Bhopal, M.P, India

¹ shahnawaz162@gmail.com

² cgupta.011@gmail.com

³ ies.abhi@gmail.com

Abstract — New approaches for active power regulation of photovoltaic (PV) inverters that do not require energy storage. As more PV power systems become networked with the electric power system, certain traditional generators that presently balance generation and load and regulate grid frequency by adjusting their active power output will be displaced. PV generators may be requested or needed to contribute to grid frequency stability and control by regulating their output power at very high levels of PV penetration. This paper provides a unique approach for predicting the maximum power available from a PV array, allowing an inverter to provide any needed reserve power for up-regulation at the lowest possible cost. It also presents a unique approach for boosting the speed at which a PV inverter may achieve a new power set point in response to a frequency event, hence improving the active power response of the inverter. Using a prototype inverter, both of these ways are experimentally validated.

Keywords — Electric vehicle, Plug-in electric vehicles, Battery charger, Charging infrastructure, Vehicle-to-grid, Grid-to vehicle, Charging methods.

I. INTRODUCTION

The solution proposed here for PV active power control (APC) avoids storage entirely and instead uses components already present in a typical grid interactive PV system, along with some additional sensors, to provide bi-directional, fast, and reliable active power support to the electric power system (EPS). Li-ion battery lifespan degradation problems are approximated and included into a battery charging optimization method in the instance of degradation-aware charging (DAC) of car traction batteries. The first control technique acknowledges that in order to supply bi-directional APC from a PV system without storage, the PV system must run below its maximum power point (MPP), which comes at a large opportunity cost. As a result, a technique of PV maximum power point estimate was developed to offer a dependable and precise power reserve for up-regulation while reducing opportunity cost (MPPE).

II. BACKGROUND AND OVERVIEW OF PV ACTIVE POWER CONTROL (APC)

Active power control of PV systems is at an early technology readiness level, but it is progressing rapidly and generating increased interest for reasons described here [1]. As the percentage of power generated by solar photovoltaic

(PV) systems grows, PV systems will be required to undertake many of the grid support activities formerly done by conventional rotating machines. PV inverters are increasingly being required to be able to export or import reactive power, ride through transient voltage and frequency events, and limit power during periods of high grid frequency. While these inverter capabilities enable for more PV grid penetration, they do not solve one of the most common criticisms of PV: its lack of active power dispatchability [2]. As a remedy to this problem, energy storage technologies are frequently advocated. Current storage technologies, on the other hand, have substantially shorter lifespans than other PV system components. Furthermore, while battery prices are reducing, they are not falling at the same rate as PV modules [3].

It is theoretically possible to eliminate this disadvantage and replace it with a new asset: distributed, cost-effective, and rapid PV-based frequency control, using APC of PV inverters. APC of PV has the potential to revolutionise frequency regulation, while also giving power reference tracking and bi-directional ramp-rate control, much as the provision of reactive power from dispersed resources is presently revolutionising the way intelligent power grids manage voltage [4], [5].

A. Frequency regulation background

The fast-changing power output of traditional grid-connected PV systems increases the moment-to-moment mismatch between load and supply, causing grid frequency oscillations and raising the demand for frequency control services [6]–[8]. One advantage of APC-capable PV inverters is that they can regulate frequency. As shown in Figure 1, the electric power sector divides frequency control into two categories: primary (on time scales of a few seconds and lower) and secondary (on time scales ranging from a few seconds to several minutes) [9], [10].

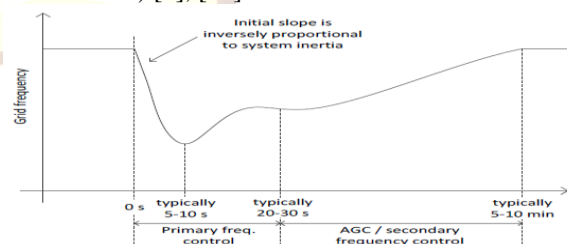


Fig. 1 Inertial, primary and secondary frequency control following a frequency disturbance at time zero. X-axis not to scale.

B. Potential benefits of APC of PV

PV-based APC may find application in at least three scenarios:

1) **Island:** The unpredictability of renewable output is particularly significant in distant, island, or islanded microgrid power systems since electricity cannot be exported or imported from surrounding networks. For example, new big PV generating facilities are needed on the island of Puerto Rico to offer primary frequency regulation and regulated power ramp-rates (both up and down). The PV industry is reacting to this need by incorporating battery systems into PV projects, which raises capital and maintenance costs dramatically. PV system frequency management can lower the amount of storage required and/or minimise battery cycling, thereby increasing battery life.

2) **Very high penetration of inverter-coupled generation:** Even on big national and continental power networks, the demand for auxiliary services such as frequency management grows as renewable energy grows. Ireland, Canada, Denmark, and Spain have all implemented wind-related frequency regulating rules as of 2012. Many transmission providers in the United States are considering enacting similar standards for wind and, ultimately, PV.

3) **Regulation markets:** When the value of frequency regulation per MW-hour exceeds the value of power from a PV plant in MWh in liberalised electricity markets, it may make economic sense for privately owned PV plant operators to provide frequency regulation services rather than operate in MPPT (maximum power point tracking) mode. The cost per MW-hour of frequency regulation is predicted to climb as the demand for frequency regulation grows. Furthermore, owing to economic development, increases in renewable energy, and electrical market liberalisation, the overall value of the frequency control industry is predicted to expand between 38 percent and 191 percent over the next decade, reaching \$56.8 billion per year by 2022.

III. REAL-TIME PV MAXIMUM POWER-POINT ESTIMATION (MPPE)

The rotational inertia of a typical PV plant is zero, thus energy storage is little. To execute PFR, synthetic inertia, or other APC activities, it must run below its maximum power point, P_{mp} , resulting in a power reserve margin that may be deployed automatically during frequency transients [1]. Typical PV inverters use one of many MPPT approaches, such as those listed above, to try to always run at the maximum power available from the PV array. Based on the irradiance incident on the array and the temperature of the PV cells, the maximum power point of a PV array fluctuates continually across a large range.

Some previously suggested MPPE algorithms, which commonly use regression analysis or neural networks, are aimed for offline PV power prediction for planning reasons [12]. These approaches can be fairly precise, but they may need more processing power than a PV inverter's integrated CPU generally provides. Other real-time calculation approaches entail assumptions that lower the PV model's

accuracy or need knowledge that isn't normally available on PV module data sheets. The MPPE approach provided here combines a number of techniques.

- 1) Offline calculation to estimate the parameters of a detailed PV cell model from data sheet values, and
- 2) Online, real-time computation of a second-order polynomial to estimate P_{mp} from irradiance and temperature.

A. MPPE method

The capacity to raise output power on demand is required for bi-directional active power regulation of PV systems without energy storage. The unique application determines the minimal amount of electricity maintained in reserve for this reason. The needed power reserve, PRES, for the PV system is assumed to be given as an input to the system in this study, for example, by power system-level or market-level regulations. The inverter-level control described here has the goal of estimating the instantaneous maximum power available, P_{mp} , and controlling the inverter to run around a power set point $P_{setPV} = P_{mp} - PRES$, as illustrated in Figure 2.

This enables the inverter to increase or decrease output power in response to variations in grid frequency.

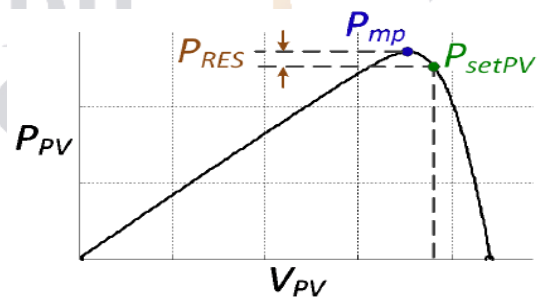


Fig. 2 The power-voltage curve of a PV array illustrating an operating point P_{setPV} below the maximum power point.

B. Droop control

Such a droop response can offer not just main frequency control, but also something like to the stabilising effect of synchronous machine inertia, thanks to the quick reaction of power electronics. While a quick droop reaction can lessen the severity of frequency events in a comparable fashion to physical inertia, it varies in three important ways:

- 1) Droop reacts to the deviation of measured grid frequency from its nominal value, whereas physical inertia responds to the first time derivative of frequency.
- 2) Physical inertia responds to local frequency instantaneously, whereas droop response will always have some short delay due to the time for the phase locked loop (PLL) to detect the frequency change and the inverter controls to take action.
- 3) Physical inertia is an inherent property of rotating machines and cannot be easily changed, whereas droop parameters can be easily adjusted at any time.

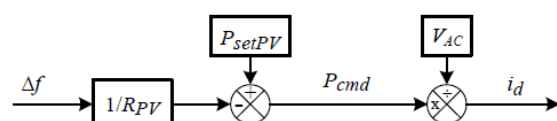


Fig. 3 Inverter power-frequency droop controller (without deadband).

C. PV APC simulation

The dynamic model of an electric power system is a basic one that captures frequency but not voltage dynamics. Figure 4 shows the EPS line-frequency response model that was employed in this study, including grid frequency dynamics. The EPS frequency dynamic model is based on the provided model, which is based on a model presented in the Western Interconnection of the United States. The grid frequency dynamics are based on the inertia, load damping, and governor droop of a reheat steam turbine, which is a prevalent kind in the United States. The total grid power and total interconnection inertia, j , have been reduced for this analysis, but the inertia constant, H , has remained the same because it is computed in per-MW terms. The model includes a single 43 MW steam turbine that may be taken offline to mimic a substantial frequency decrease, in addition to the huge steam turbine that represents the "rest of the interconnection" (ROI).

D. MPPE experimental demonstration

The experimental validation of the P_{mp} prediction approach is shown in Figure 5. By comparing the observed output power of a 3 kW commercially available PV inverter in MPPT mode to the maximum power, P_{mp} , projected using measured irradiance and temperature, the approach was validated [13].

A PV array of 26 Solarex 110S modules supplied power to the PV inverter. These are the identical PV modules that were utilised in the previous example calculation. The DC-AC conversion efficiency, 0.95, was assumed. Except for very quick cloud transients, when the inverter's MPPT algorithm appears to fail briefly, the anticipated power (blue trace) matches the observed power (red trace) quite well. For such a modest PV system, the effect of the low-pass filter is insignificant on the time scale depicted in Figure 5.

The sbRIO's real-time CPU was used to implement the active power controls. LabView's Real-Time graphical programming language was used to create the control code. The real-time processor interacts with the FPGA's low-level code, receiving data on frequency, RMS AC voltage and current on each phase, DC voltage and current, and other parameters [14].

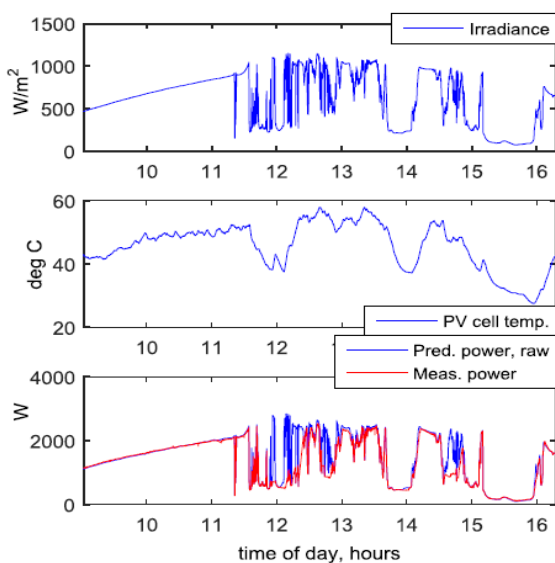


Fig. 5 Preliminary experimental validation of the MPPE method. The top two plots show measured irradiance and PV cell temperature. The bottom plot shows the predicted output power and the measured output power of a commercial inverter operating in MPPT mode.

To regulate active power in APC mode, the DC bus voltage is adjusted to the desired place on the PV array's I-V curve. As a result, the low-level controls are set to DC voltage control mode, and the real-time processor's active power control code delivers DC voltage commands to the FPGA. The FPGA communicates with the sbRIO's analogue to digital converters (ADCs). Solar irradiance and PV module temperature readings were sent into two unused ADCs, which were then processed in the FPGA before being fed into the real-time code.

IV. RAPID ACTIVE POWER OF CONTROL PV SYSTEMS

To modulate output power, a typical PV inverter must regulate its DC input voltage to an appropriate point on the PV array's power voltage (P-V) curve, as shown in Figure 7. A typical PV inverter does not incorporate stored energy above that required to maintain stable operation over a single line cycle (or less). With solar irradiation and PV module temperature, the P-V curve varies continually [15]. Furthermore, the inverter controller often has no means of knowing where it is on the P-V curve in relation to the maximum power point or open-circuit voltage. The purpose of traditional PV inverter design is to optimise the system's instantaneous output power to maximise energy production, a technique known as maximum power point tracking (MPPT). As a result, the majority of commonly used methods of controlling output power are heuristic methods like "perturb and observe," in which the PV array voltage (or current) is perturbed from its operating point, the new operating point is allowed to stabilise, the change in power is measured, and the operating point is then perturbed in a direction that depends on whether the power went up or down. Because this is a sluggish operation, it is not suitable for rapidly adjusting output power to a new operating point for fast frequency support.

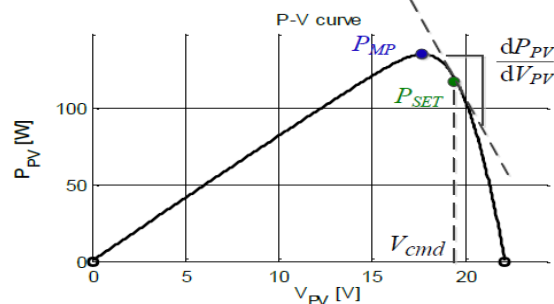


Fig. 7 The power-voltage curve of a PV array illustrating a single operating point, P_{SET} , and the voltage V_{cmd} need to achieve that operating point. The local slope of the curve at V_{cmd} is also illustrated.

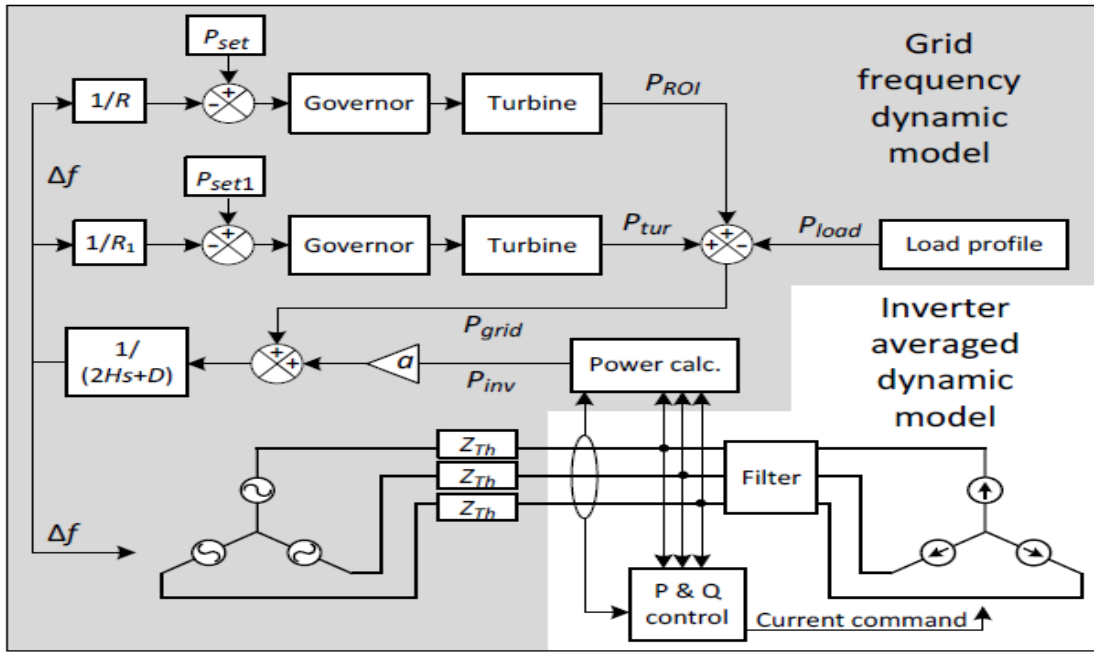


Fig 4: Line-frequency response model of grid and PV inverter.

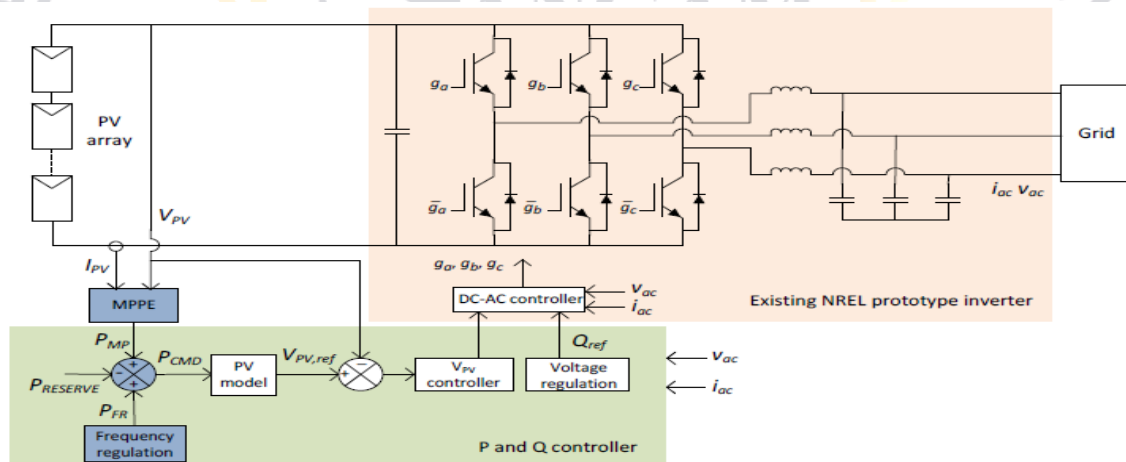


Fig 6: Experimental setup for hardware validation of MPPE method.

A. Candidate active power control methods

The first technique of active power control addressed here would use the equation to generate a voltage command from a desired power command using the instantaneous slope of the P-V curve, as shown in Figure 7.

$$V_{cmd} = V_{PV} + \frac{P_{cmd} - P_{PV}}{dP_{PV}/dV_{PV}}$$

The inverter controller would estimate the slope dP_{PV}/dV_{PV} from minor perturbations in the operating voltage V_{PV} on a regular basis. This approach could be useful for responding to lower-frequency events that only need a slight change in output power, as long as the new operating point is in the area where $P_{PV}(V_{PV})$ is well approximated by

its tangent. The most important frequency occurrences, on the other hand, are the ones that need the inverter to deliver all or virtually all of its reserve power to the grid. These are occasions when a response based on a small-signal approximation of the P-V curve will be severely erroneous, notably underestimating necessary voltage change for under frequency events and overestimating required change in voltage for over frequency events.

B. Candidate active power control

Given the difficulties found with earlier approaches, it was decided to create a three-dimensional lookup table (LUT) that would be stored in the inverter and used to estimate the value of V_{cmd} that would result in the required power output: $V_{PV} = g3(P_{PV}, G, T)$. This LUT should cover

the complete projected power, module temperature, and irradiance working range. To minimise the size of the table required to achieve the requisite precision, the LUT can be interpolated using trilinear interpolation. Despite this, the size of the LUT in each dimension was carefully studied in order to provide an accurate table of manageable size. Because the LUT is three-dimensional, it has the potential to grow rather enormous.

Because the gradients dP_{PV}/dT and dV_{PV}/dG are rather smooth across the working area, the granularity of the LUT in the temperature and irradiance dimensions can be quite coarse. Figure 8 shows this, and it's also intuitive: when module temperature or irradiance rises, one wouldn't expect very non-uniform variations in the P-V curve of a PV module.

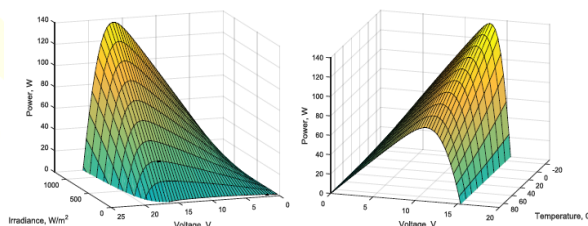


Fig 8: PV power as a function of irradiance and voltage at constant cell temperature (left), and as a function of cell temperature and voltage at constant irradiance (right).

C. Experimental demonstration of MPPE and rapid APC

The RAPC approach was validated using a prototype inverter with MPPE and a LUT for quick APC. A Yokogawa PZ4000 power analyzer was used to record the inverter's reaction after the grid simulator in the test setup was designed to simulate a range of frequency occurrences. The PZ4000 captured voltage and current waveforms, which were then processed to determine frequency, actual power, and other parameters. During the experiments, the sbRIO controller also logged its internal control signals. Control and measured signals were displayed on the same time axis once the data files were synced [16].

Figure 9 depicts the reaction of the prototype inverter to a frequency event with a depths of 50 Hz and a ROCOF of 2 Hz/s, which is quicker than what would be seen on a big interconnected power system but feasible for a system like Ireland's. The inverter was set to MPPE mode, with 0.8 kW of reserve power and a 5% droop slope (which means that a frequency shift of 5% of the nominal frequency, or 3 Hz, will result in a change of 100% of the inverter's nominal power). Although the machine reaction is hundreds of magnitude slower than the inverter response illustrated above, a 5% droop slope is a common number utilised in synchronous machines

providing main frequency control. The programmed droop slope lacked a deadband, which is typical in conventional generators, although it could simply be adjusted to include one.

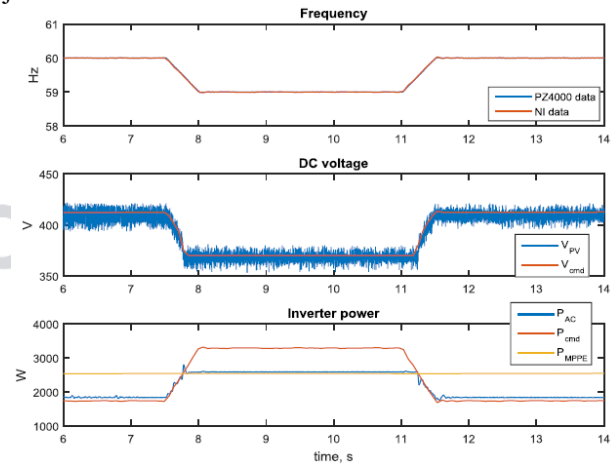


Fig 9: Response of the prototype inverter to a frequency event with a nadir of 50 Hz and a 2 Hz/s ROCOF.

To synchronise the test data from the two recording devices, the PZ4000 frequency trace and the inverter's internal frequency measurement (labelled "NI data" in the frequency plot) were utilised. Almost instantly, the inverter responds to the frequency incident. Both the measured DC voltage V_{PV} and the measured AC power P_{AC} follow the requested values, V_{cmd} and P_{cmd} , quite closely. The AC power does not, of course, exceed the projected maximum power available, P_{MPPE} , confirming the MPPE approach. Measurement noise, switching frequency ripple, and DC voltage ripple at a multiple of the line frequency (presumably owing to a minor imbalance between phases) make up the high frequency component of the DC voltage measurement. Figure 10 shows how the measured power trails the required power by less than 20 milliseconds during the first section of the frequency event.

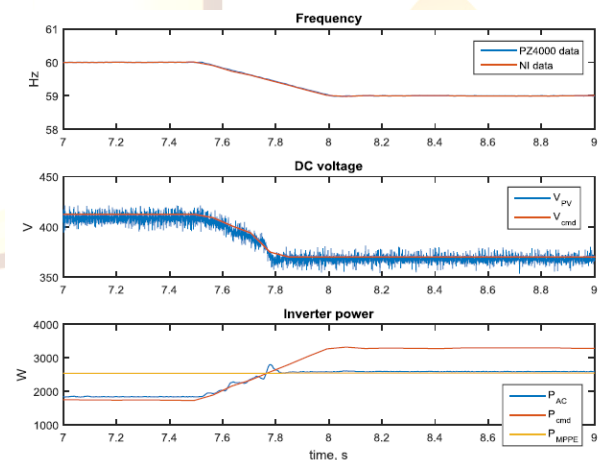


Fig 10: Zoomed in response of the prototype inverter to a frequency event with a depths of 50 Hz and a 2 Hz/s ROCOF.

V. BATTERY LIFETIME COMPARISONS

Five days of commuting of 26-40 km (16-25 miles) round-way, one longer trip of 65 km (40 miles), and one day on which the car was not utilised were chosen as a typical driving week. These details included the driving SOC profiles, charging time frames, and beginning SOC values for each charge. Three different battery sizes were simulated: the Prius' 3.5 kWh battery, a 19 kWh battery, and a bigger 35 kWh battery. Scaling the Prius data produced hypothetical simulated SOC profiles for the bigger batteries.

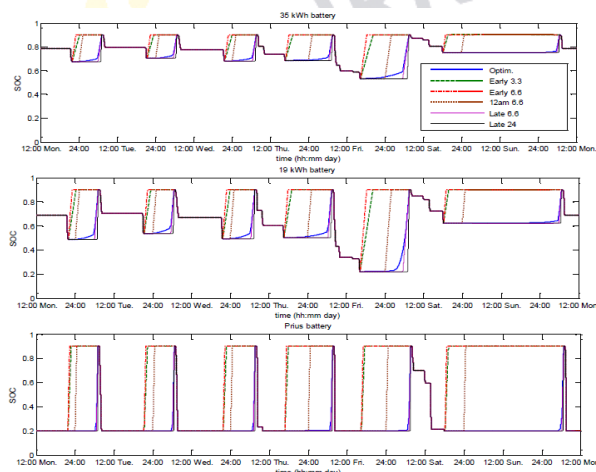


Fig 11: Weekly SOC profiles for three battery sizes under various charging scenarios.

According to the suggested charge optimization approach, quick charging reduces battery deterioration, therefore it would most likely choose a charge profile comparable to one of the two early charging scenarios. Because the optimization approach chooses to charge late in the available window, it is the most comparable to the two late charging situations.

VI. CONCLUSION

This concept to PV maximum power point estimate using active power control is a rapid, accurate, and empirically confirmed approach. This approach uses typical PV module data sheet values to create a second-order polynomial that predicts the maximum power point of a PV system based on observed irradiance and PV module temperature using numerical modelling and linear regression. The polynomial coefficients are computed offline and stored in the PV inverter's controller, allowing the controller to predict the PV array's highest power point in real time. Once the maximum power point has been determined, the PV inverter can operate with a commanded power reserve, allowing active power to be modulated for a variety of grid support functions and ancillary services such as primary and secondary frequency regulation, synthetic inertia, fast frequency response (FFR), and other services.

It is a method for managing the DC voltage of a PV array in order to obtain a desired output power in a few AC line cycles. Typical ways of managing the output power of a PV array are slower, making them ineffective for responding to grid frequency contingency events, where time is crucial. The three-dimensional lookup table of the PV array voltage required to deliver a certain output power at a given irradiance and PV module temperature is stored in the rapid active power control (RAPC) system provided here. Using measured irradiance and temperature, this lookup table may be stored in the controller of a PV inverter and interpolated to transform power commands into DC voltage commands.

The RAPC lookup table is built offline using PV module data sheet parameters, same as the MPPE approach.

REFERENCES (SIZE 10 & BOLD)

- [1] A. Hoke and D. Maksimovic, "Active power control of photovoltaic power systems," in *2013 1st IEEE Conference on Technologies for Sustainability (SusTech)*, 2013, pp. 70–77.
- [2] A. Hoke and P. Komor, "Maximizing the benefits of distributed photovoltaics," *Electr. j.*, vol. 25, no. 3, pp. 55–67, 2012.
- [3] "Electricity Storage Technology Brief," International Energy Agency Energy Technology Systems Analysis Programme (IEA-ETSAP) and International Renewable Energy Agency (IRENA), Apr. 2012.
- [4] Stetz, T., Yan, W., and Braun, M., "Voltage Control in Distribution Systems with High Level PV-Penetration - Improving Absorption Capacity for PV Systems by Reactive Power Supply-," in *25th European Photovoltaic Solar Energy Conference and Exhibition / 5th World Conference on Photovoltaic Energy Conversion*, Valencia, Spain, 2010.
- [5] P. M. S. Carvalho, P. F. Correia, and L. A. F. M. Ferreira, "Distributed Reactive Power Generation Control for Voltage Rise Mitigation in Distribution Networks," *IEEE Trans. Power Syst.*, vol. 23, no. 2, pp. 766–772, May 2008.
- [6] H. Asano, K. Yajima, and Y. Kaya, "Influence of photovoltaic power generation on required capacity for load frequency control," *Energy Convers. IEEE Trans. On*, vol. 11, no. 1, pp. 188–193, 1996.
- [7] H. Bevrani, A. Ghosh, and G. Ledwich, "Renewable energy sources and frequency regulation: survey and new perspectives," *Renew. Power Gener. IET*, vol. 4, no. 5, pp. 438–457, 2010.
- [8] j. H. Eto, "Use of frequency response metrics to assess the planning and operating requirements for reliable integration of variable renewable generation," LBNL-4142E, 2011.
- [9] Y. G. Rebours, D. S. Kirschen, M. Trotignon, and S. Rossignol, "A survey of frequency and voltage control ancillary services—part II: economic features," *Power Syst. IEEE Trans. On*, vol. 22, no. 1, pp. 358–366, 2007.
- [10] j. Aho, A. Bucksan, j. Laks, P. Fleming, Y. jeong, F. Dunne, M. Churchfield, L. Pao, and K. johnson, "A tutorial of wind turbine control for supporting grid frequency through active power control," in *American Control Conference (ACC)*, 2012, 2012, pp. 3120–3131.
- [11] H. T. Ma and B. H. Chowdhury, "Working towards frequency regulation with wind plants: Combined control approaches," *IET Renew. Power Gener.*, vol. 4, no. 4, pp. 308–316, jul. 2010.
- [12] Khan S, Gupta C. An optimization techniques used for economic load dispatch. *Int j Adv Technol Eng Res (IjATER)*. 2014;4(4).



- [13] A. Tiwari and C. Gupta, "A Fuzzy Logic Controller Used for Governing the Speed of DC Motor."
- [14] R. Kumar; C Gupta, "REVIEW OF SHUNT ACTIVE POWER FILTERS CONTROL STRATEGIES FOR ELIMINATION OF HARMONICS," *IjESM*, vol. 8, no. 2, pp. 225–230, 2018, doi: 10.17148/ijreice/ncaee.2017.03.
- [15] P. Verma and M. T. Student, "Three Phase Grid Connected Solar Photovoltaic System with Power quality Analysis." *Shodh Sangam*, pp. 111–119, 2018, [Online]. Available: <http://www.shodhsangam.rkdf.ac.in/papers/suvenir/111-119-Privnka.pdf>.
- [16] A Hridaya; C Gupta, "AN OPTIMIZATION TECHNIQUE USED FOR ANALYSIS OF A HYBRID SYSTEM ECONOMICS," *Int. j. Curr. Trends Eng. Technol.*, vol. 1, no. 6, pp. 136–143, 2015, [Online]. Available: https://www.academia.edu/22728404/AN_OPTIMIZATION_TECHNIQUE_USED_FOR_ANALYSIS_OF_A_HYBRID_SYSTEM_ECONOMICS.

